

## Flux pinning by regular nanostructures in Nb thin films: Magnetic *vs.* structural effects

M. I. MONTERO<sup>1</sup>, J. J. AKERMAN<sup>2</sup>, A. VARILCI<sup>3</sup> and I. K. SCHULLER<sup>1</sup>

<sup>1</sup> *Physics Department, University of California San Diego - La Jolla, CA 92093, USA*

<sup>2</sup> *Motorola Labs - 7700 S. River Parkway, Tempe, AZ 85284, USA*

<sup>3</sup> *Department of Physics, Faculty of Arts and Sciences, Karadeniz Technical University 61080 Trabzon, Turkey*

(received 11 June 2002; accepted in final form 17 April 2003)

PACS. 74.25.Qt – Vortex lattices, flux pinning, flux creep.

PACS. 74.25.Sv – Critical currents.

**Abstract.** – Periodic pinning effects in indented Nb films and Nb films with rectangular arrays of submicrometric Ni dots were studied. The indented samples consisted of Nb film deposited on top of Si substrates patterned with rectangular arrays of nanoholes. Pinning effects can be observed in the evolution of resistivity and critical current with the applied magnetic field, showing the same qualitative behavior, for both types of samples. The main difference between them is that the matching effects are more pronounced in the samples with magnetic dots. The analysis and comparison of these results allows determining the pinning as due to superconductivity suppression around the nanostructures (indentations or dots) due to a thickness reduction. For the samples with magnetic dots, this suppression of superconductivity is reinforced by the magnetic proximity effect.

*Introduction.* – Recent advances in nano-lithographic techniques have generated a renewed interest in the study of vortex statics and dynamics in superconductors with periodic pinning arrays. Techniques such as e-beam [1,2], laser-interference [3], or X-ray lithography [4] make it possible to create regular structures with sizes of the order of relevant length scales such as the coherence length and the penetration depth of low- $T_c$  superconductors. Systems with arrays of magnetic dots [5–8] or holes [9–11] show commensurability effects between the vortex lattice and the pinning center array, and novel geometrical configurations of the vortex lattice are stabilized [12]. The existence of novel plastic flow phases, which are not observed in systems with random pinning centers, was predicted by numerical simulations [13,14] and is observed here. An interesting technological application for periodic pinning arrays is the reduction of low-frequency noise in SQUIDs [15,16].

In the case of magnetic dots, the commensurability effects in superconducting thin films have been studied as a function of different parameters such as array geometry [5,7,17,18], and magnetic state [19], etc. The experimental results show that there is a dependence of the periodic pinning effect on the properties of the vortex lattice (*i.e.* vortex-vortex interactions, elastic energy and vortex velocity) and also on the dot characteristics (*i.e.* dot size, distance between dots, magnetic character of the dot material, etc.). However, there is still not a good

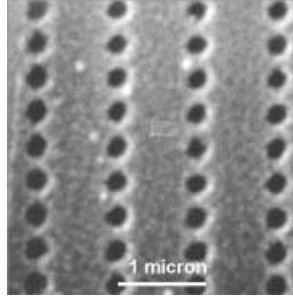


Fig. 1 – SEM picture of an indented film of Nb. The indentations are 300 nm in diameter and positioned in a rectangular array of  $400 \times 900 \text{ nm}^2$ .

understanding of the nature of the main pinning mechanisms by the magnetic dots and the role of the structural effects, such as the corrugation.

Our aim in the present work is the comparison between pinning due to purely structural mechanisms and that due to the magnetic nature of the dots. The effect of the corrugation on the vortex pinning was studied in indented Nb films. These samples consist of a Nb film deposited on top of a Si substrate with a rectangular array of nanoholes. The magnetic effects were studied in Nb films deposited on Si substrates with rectangular arrays of Ni dots. In this case we have the additional effects due to the corrugation induced by the underlying dots.

*Experimental.* – Rectangular arrays of submicrometric Ni dots were fabricated by e-beam lithography on Si(100) substrates; a detailed description of the process can be found in ref. [20]. On top of the dot array, a 75 nm thick Nb film is deposited by sputtering.

The indented samples were prepared by sputtering a Nb film on top of pre-patterned Si(100) substrates. Arrays of holes were made in the Si substrates using e-beam lithography and reactive ion etching. Figure 1 shows the typical aspect of the indentations (300 nm in diameter) in the Nb film. While the exact nature of the samples prepared this way has not

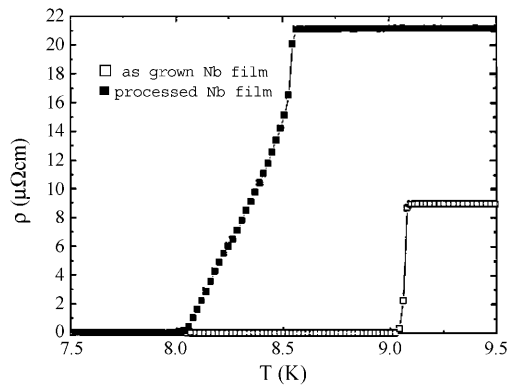


Fig. 2

Fig. 2 – Resistivity *vs.* temperature for two pieces of the same 85 nm thick Nb film.

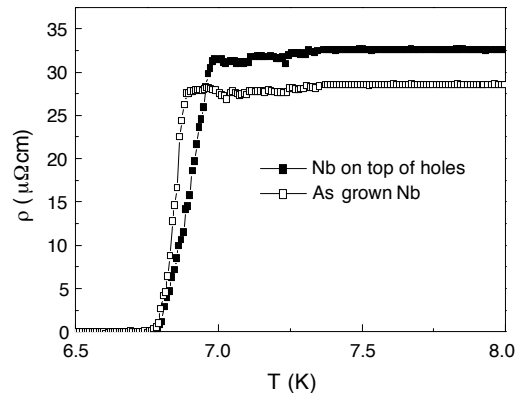


Fig. 3

Fig. 3 – Resistivity *vs.* temperature for two pieces of the same 80 nm thick Nb film.

TABLE I – *Sample characteristics.  $t_{\text{Nb}}$  is the Nb film thickness, the penetration depth and the coherent length are estimated for  $T/T_c = 0.94$  for the indented film and  $T/T_c = 0.95$  for the Ni dot sample.*

Sample	$t_{\text{Nb}}$ (nm)	$T_c$ (K)	$\Delta T_c$ (K)	$\lambda$ (nm)	$\xi$ (nm)
Indented film	80	6.94	0.12	457	33
Ni dots	75	8.2	0.093	500	36

been unequivocally determined, we believe them to be continuous with indentations, since the lithography produces rather shallow sloped holes.

The above process induces film corrugation without any undesirable degradation of the Nb, in contrast to the process where holes are created by direct patterning of the Nb film. This degradation can be observed in fig. 2 where the resistance *vs.* temperature is shown for two pieces of the same Nb film with a thickness of 85 nm. One piece is measured as grown, while the other went through the whole process for the e-beam lithography. Clearly, the critical temperature decreases, the superconducting transition broadens significantly and the resistivity increases by a factor of two. In the case of Nb films deposited on top of the pre-patterned Si substrates, degradation is much smaller, as shown in fig. 3. The resistance *vs.* temperature for two zones of the same 80 nm thick Nb film, one measured on top of the arrays of holes and the other as grown, is almost the same. Note that the differences in  $T_c$  between the “as grown” Nb samples in figs. 2 and 3 may be related to the different thicknesses.

For the transport measurements a 40  $\mu\text{m}$  bridge is defined using standard optical lithography and reactive ion etching. The measurements are performed in a helium flow cryostat, with the applied field perpendicular to the substrate plane and the current applied parallel to the long side of the rectangular array cell.

*Results.* – The measurements presented below have been made on two samples. The first sample consists of a 75 nm thick Nb film covering a rectangular ( $400 \times 900 \text{ nm}^2$ ) array of Ni dots having a thickness of 40 nm and a diameter of 300 nm. The second sample is an 80 nm thick Nb film deposited on top of a Si substrate with a rectangular ( $400 \times 900 \text{ nm}^2$ ) array of holes with a diameter of 300 nm and a depth of 150 nm (see table I for detailed sample characteristics).

Figures 4 and 5 show the field dependence of the resistivity in the mixed state for the sample with Ni dots ( $T = 0.95T_c$ ,  $J = 3.3 \text{ kA/cm}^2$ ) and the indented film ( $T = 0.94T_c$ ,  $J = 3.1 \text{ kA/cm}^2$ ), respectively. These measurements were taken by applying a current slightly above the critical current. Two types of minima can be observed in the magneto-resistivity: i) narrow and deep at low fields; ii) broad and shallow at higher fields (above 150 G for the indented film and 200 G for the Ni dot sample). The detailed study of the position of the minima ( $B_n$ ) reveals two different periodicities ( $\Delta B$ ) in the spacing of the minima, as shown in fig. 6. In the case of magnetic dots, these two different kinds of minima in the magnetoresistance have been previously explained by a matching between the vortex lattice and the rectangular dot array at low fields, followed by a reconfiguration to a more isotropic square geometry at higher fields [12]. Now we observed this vortex lattice reconfiguration in the indented film, we must mention that samples previously studied where the array of holes were prepared using a pre-patterned  $\text{SiO}_2$  layer did not show periodic oscillations in the magnetoresistance. At low fields, the periodicity of the minima can be determined from the pinning center density and in the case of a rectangular array it is given by  $\Delta B_{\text{rect}} = \Phi_0/cd$ , where  $\Phi_0$  is the flux quantum (the magnetic flux in each vortex), and  $c$  and  $d$  are the lattice parameters of the rectangular pinning array. In table II we compare the theoretical and experimental ( $\Delta B_{\text{low}}$ ) values obtained for both samples. In the high-field regime, the

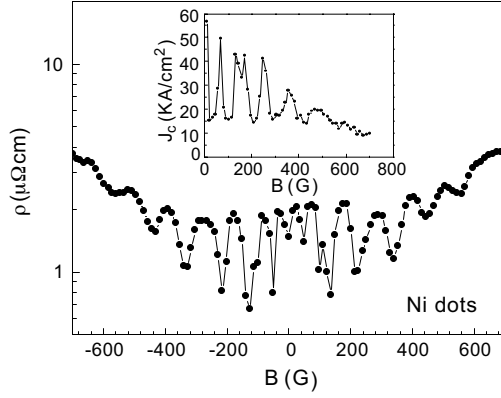


Fig. 4

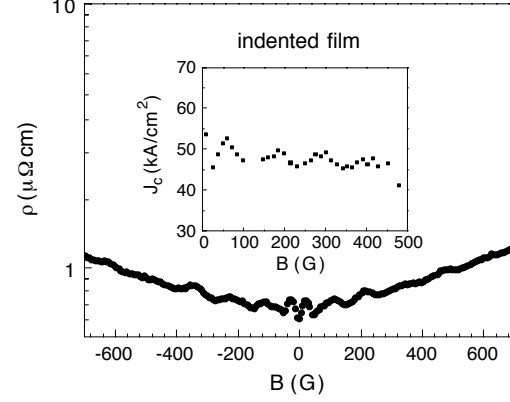


Fig. 5

Fig. 4 – Resistivity *vs.* applied field for Ni dot sample measured at  $T/T_c = 0.95$  with a current density of  $3.3 \text{ kA/cm}^2$ . Inset: evolution of the critical current with the applied field.

Fig. 5 – Resistivity *vs.* applied field for indented film measured at  $T/T_c = 0.94$  with a current density of  $3.1 \text{ kA/cm}^2$ . Inset: evolution of the critical current with the applied field.

periodicity is much larger and similar to the theoretically expected value for a square vortex lattice with a parameter corresponding to the short side of the rectangular array  $\Delta B_{\text{sq}} = \Phi_0/c^2$  (see table II).

Although both samples present the same qualitative behavior, there are several differences between the indented film and the sample with magnetic dots. While the reconfiguration of the vortex lattice in the indented film takes place between the second (the peak in the resistivity is not completely developed due to the beginning of the reconfiguration) and third matching field (see fig. 6), the magnetic dot sample shows an extended low-field range with sharp minima

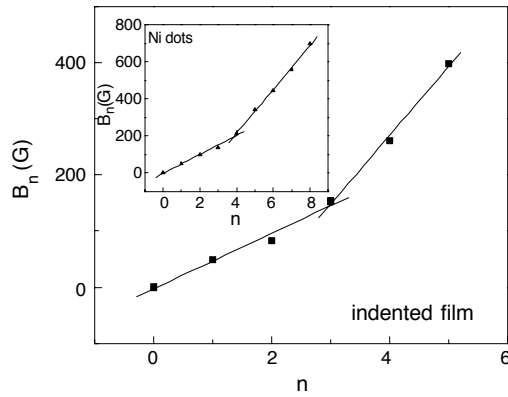


Fig. 6

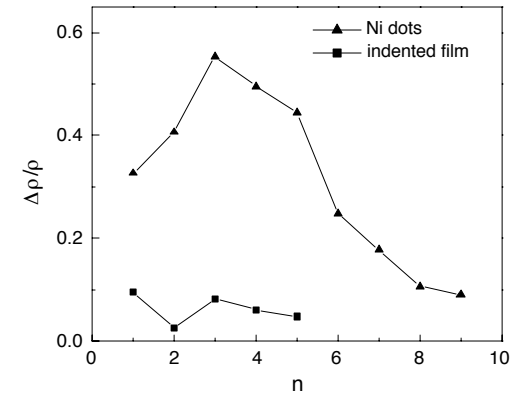


Fig. 7

Fig. 6 – Matching fields *vs.* index number for indented film as extracted from fig. 4. Inset: matching fields *vs.* index number for the sample with Ni dots. Solid lines are linear fits to the data.

Fig. 7 – Normalized resistivity change *vs.* index number.

TABLE II – *Experimental and theoretical periodicities for the matching peaks at low ( $\Delta B_{\text{low}}$ ) and high ( $\Delta B_{\text{high}}$ ) field.*

Sample	$\Delta B_{\text{low}}$ (G)	$\Delta B_{\text{high}}$ (G)
Indented film	$49 \pm 5$	$123 \pm 8$
Ni dots	$51 \pm 3$	$119 \pm 3$
Theoretical values	$58 \pm 2$	$129 \pm 5$

persisting up to the fourth matching field. The number of minima after the reconfiguration is also higher in the case of the magnetic dot sample. Another difference can be observed in the normalized resistivity change  $\Delta\rho/\rho$  at each matching field (see fig. 7), where  $\Delta\rho$  is defined by the resistivity minimum at each matching field subtracted from the background resistivity  $\rho$  given by an interpolation between the maxima of the resistivity in between the matching fields.  $\Delta\rho/\rho$  for the sample with Ni dots increases with the matching field until the reconfiguration of the vortex lattice takes place and then decreases monotonically. For the indented film  $\Delta\rho/\rho$  decreases with increasing matching field order after the reconfiguration; at low fields we can observe only the first matching peak and the normalized resistivity change has a minimum at the second matching field because the peak in the resistivity is not completely developed due to the beginning of the reconfiguration (see fig. 5). The evolution of the normalized resistivity with the matching field order presents the same qualitative dependence for both samples; however, the changes of the normalized resistivity are more pronounced in the magnetic dot sample.

The appearance of minima in dissipation, for both samples, is present only for a limited range of currents and temperatures. At high currents, the resistivity is similar to that of the normal state. When the current is reduced, the periodic minima appear; however, a further decrease of the current smears out the periodic structure. But we can still observe the differences between both samples in the reconfiguration of the vortex lattice and in the normalized resistivity change at each matching field when we change the temperature of measurement.

The evolution of the critical current with the applied magnetic field presents maxima at the same field values as the minima in the resistivity curves, for both samples (see insets of figs. 4 and 5). We can even observe the vortex lattice reconfiguration, and similarly to the case of the resistivity minima, the critical current maxima are sharp and narrow before the reconfiguration and broad and shallow at higher fields. The oscillations of the critical current are also more pronounced in the case of the sample with magnetic dots, in good correlation with the measurements of magnetoresistance.

*Discussion.* – From the observed matching effects it is clear that the Ni dots and the corrugation of the indented film act qualitatively in the same way as pinning centers for the vortices. The main difference is the strength of the matching effects (in the static and dynamical properties), which are less pronounced in the indented film. The question hence arises whether the magnetism of the dots plays a role in these more pronounced effects.

In the case of the indented film it is clear that the pinning mechanism is the corrugation of the film. The deposition of the Nb film on top of the arrays of holes creates areas in the film with reduced thickness. This reduced thickness can pin a vortex, since when a vortex is positioned at the constriction of the superconducting film the loss in condensation energy due to the normal conducting vortex core is minimized. Besides, it is well known that the critical temperature depends on the superconducting film thickness and the Nb films used

in this study have thicknesses where this effect becomes relevant [21–23]. Indeed, the first measurements of vortex matching effects in type-II superconductors were done in granular films with periodic thickness modulation [24].

In the case of the sample with Ni dots, the corrugation of the Nb film deposited on top of the dots provides a possible source of pinning. The film has a reduced thickness along the perimeter of the dot where the superconductivity can be suppressed locally. Indeed, previous experimental results showed periodic pinning effects in samples with non-magnetic dots [5, 18, 19], but in all cases the effects are less pronounced than in samples with magnetic dots.

A possible source of magnetic vortex pinning is the stray field in multidomain magnetic dots which can suppress superconductivity locally [19, 25, 26]. In this case, the pinning should depend on the magnetic state and history of the ferromagnetic dots. However, the results presented in this paper show no dependence of the magnetic history of the dots, since we obtained the same results if the samples were previously magnetized with a 1 T field. Another possibility for pinning is the depression of superconductivity by the perpendicular stray field [19], the perpendicular moment in a magnetic vortex state [27] and/or the local suppression of superconductivity above the dots due to the magnetic proximity effect. The temperature dependence of the critical current density in Nb samples with Ni dots suggests [28] two possible magnetic mechanisms, the proximity effect and a “dirty” interface between the Ni dot and the Nb film in which the dot does not perturb the superconducting properties of the Nb film, so the pinning occurs via a magnetic interaction with an unperturbed vortex. However, the pinning effects observed in samples with non-magnetic dots and the fact that the static and dynamical pinning effect for the indented film showed the same qualitative behavior as in the sample with magnetic dots lead us to suggest that the suppression of superconductivity by these magnetic proximity effects is the main magnetic pinning mechanism.

*Conclusions.* – We have compared the pinning effects in indented Nb films with Nb films with rectangular arrays of submicrometric Ni dots. The Nb films are deposited on top of a substrate with a pre-patterned array of nanoholes or on arrays of submicrometric Ni dots prepared using e-beam lithography.

The evolution of the resistivity and the critical current with applied field shows the same qualitative behavior for both types of samples. The reconfiguration of the vortex lattice from a rectangular (at low fields) to a square (at higher fields) configuration takes place at a lower field in the indented film. The main difference in the pinning in both types of sample is the pinning strength, which is more pronounced in the samples with magnetic dots. These results can be understood in terms of local suppressions of superconductivity in the films. In the case of the indented films, this suppression is due to the film corrugation, while in the case of the films with magnetic dots, the vortex pinning due to the film corrugation is reinforced by the destruction of superconductivity through the magnetic proximity effect.

\* \* \*

This work was supported by the US National Science Foundation. We thank A. HOFFMANN, J. L. VICENT for useful conversations and F. SHARIFI and M.-C. CYRILLE for useful discussions about the etching of Si. MIM thanks the Spanish Secretaría de Estado de Universidades e Investigación for supporting her stay at UCSD, and AV thanks The Scientific and Technical Research Council of Turkey (TUBITAK) for financial support.

## REFERENCES

- [1] KIRK K. J., CHAPMAN J. N. and WILKINSON C. D. W., *Appl. Phys. Lett.*, **71** (1997) 539.
- [2] SMYTH J. F., SCHULTZ S., FREDKIN D. R., KERN D. P., RISHTON S. A., SCHMID H., CALI M. and KOEHLER T. R., *J. Appl. Phys.*, **69** (1991) 5262.
- [3] SPALLAS J. P., HAWRYLUK A. M. and KANIA D. R., *J. Vac. Sci. Technol. B*, **13** (1995) 1973.
- [4] ROUSSEAU F., DECANINI D., CARCENAC F., CAMBRIL E., RAVET M. F., CHAPPERT C., BARDOU N., BARTENLIAN B. and VEILLET P., *J. Vac. Sci. Technol. B*, **13** (1995) 2787.
- [5] JACCARD Y., MARTÍN J. I., CYRILLE M.-C., VÉLEZ M., VICENT J. L. and SCHULLER I. K., *Phys. Rev. B*, **58** (1998) 8232.
- [6] FASANO Y., HERBSOMMER J. A., DE LA CRUZ F., PARDO F., GAMMEL P. L., BUCHER E. and BISHOP D. J., *Phys. Rev. B*, **60** (1999) R15047.
- [7] MORGAN D. J. and KETTERSON J. B., *Phys. Rev. Lett.*, **80** (1998) 3614.
- [8] TERENTIEV A., WATKINS D. B., DE LONG L. E., MORGAN D. J. and KETTERSON J. B., *Physica C*, **324** (1999) 1.
- [9] BAERT M., METLUSHKO V. V., JONCKHEERE R., MOSHCHALOV V. V. and BRUYNSEAEDE Y., *Phys. Rev. Lett.*, **74** (1995) 3269.
- [10] ROSSEEL E., VAN BAELE M., BAERT M., JONCKHEERE R., MOSHCHALOV V. V. and BRUYNSEAEDE Y., *Phys. Rev. B*, **53** (1996) R2983.
- [11] METLUSHKO V. V., WELP U., CRABTREE G. W., ZHANG Z., BRUECK S. R. J., WATKINS D. B., DE LONG L. E., ILIC B., CHUNG K. and HESKETH P. J., *Phys. Rev. B*, **59** (1999) 603.
- [12] MARTÍN J. I., VÉLEZ M., HOFFMANN A., SCHULLER I. K. and VICENT J. L., *Phys. Rev. Lett.*, **83** (1999) 1022.
- [13] REICHHARDT C., OLSON C. J. and NORI F., *Phys. Rev. Lett.*, **78** (1997) 2648.
- [14] REICHHARDT C., OLSON C. J. and NORI F., *Phys. Rev. B*, **57** (1998) 7937.
- [15] SELDERS P. and WÖRDENWEBER R., *Appl. Phys. Lett.*, **76** (2000) 3277.
- [16] SELDERS P. and WÖRDENWEBER R., *IEEE Trans. Appl. Supercond.*, **11** (2001) 928.
- [17] MARTÍN J. I., VÉLEZ M., NOGUÉS J. and SCHULLER I. K., *Phys. Rev. Lett.*, **79** (1997) 1929.
- [18] HOFFMANN A., PRIETO P. and SCHULLER I. K., *Phys. Rev. B*, **61** (2000) 6958.
- [19] VAN BAELE M. J., TEMST K., MOSHCHALOV V. V. and BRUYNSEAEDE Y., *Phys. Rev. B*, **59** (1999) 14674.
- [20] MARTÍN J. I., JACCARD Y., HOFFMANN A., NOGUÉS J., GEORGE J. M., VICENT J. L. and SCHULLER I. K., *J. Appl. Phys.*, **84** (1998) 411.
- [21] BANERJEE I. and SCHULLER I. K., *J. Low Temp. Phys.*, **54** (1984) 501.
- [22] MAYADAS A. F., LAIBOWITZ R. B. and CUOMO J. J., *J. Appl. Phys.*, **43** (1972) 1287.
- [23] WOLF A., KENNEDY J. J. and NISENOFF M., *J. Vac. Sci. Technol.*, **13** (1976) 145.
- [24] DALDINI O., MARTINOLI P., OLSEN J. L. and BENER G., *Phys. Rev. Lett.*, **32** (1974) 218.
- [25] NOZAKI Y., OTANI Y., RUNGE K., MIYAJIMA H., PANNETIER B., NOZIÈRES J. P. and FILLION G., *J. Appl. Phys.*, **79** (1996) 8571.
- [26] OTANI Y., PANNETIER B., NOZIÈRES J. P. and GIVORD D., *J. Magn. & Magn. Mater.*, **126** (1993) 622.
- [27] SHINJO T., OKUNO T., HASSDORF R., SHIGETO K. and ONO T., *Science*, **289** (2000) 930.
- [28] MARTÍN J. I., VÉLEZ M., HOFFMANN A., SCHULLER I. K. and VICENT J. L., *Phys. Rev. B*, **62** (2000) 9110.